Tuning the properties of molybdenum oxide on Al2O3/NiAl(110) metal versus oxide deposition

Mom, R.V.; Rost, M.J.; Frenken, J.W.M.; Groot, I.M.N.

THE JOURNAL OF PHYSICAL CHEMISTRY C

Article

pubs.acs.org/JPCC

Tuning the Properties of Molybdenum Oxide on Al_2O_3/NiAl(110): Metal versus Oxide Deposition

Rik V. Mom,*[,†] Marcel J. Rost,[†] Joost W. M. Frenken,[†,‡] and Irene M. N. Groot[†,§]

[†]Huygens-Kamerlingh Onnes Laboratory, Niels Bohrweg 2, 2333 CA Leiden, The Netherlands

[‡]Advanced Research Center for Nanolithography, Science Park 104, 1098 XG Amsterdam, The Netherlands

[§]Gorlaeus Laboratories, Einsteinweg 55, 2333 CC Leiden,The Netherlands

Supporting Information

ABSTRACT: To investigate how the properties of model mixed metal oxide catalysts can be influenced by the choice of evaporating species during physical vapor deposition, we have compared MoO_x on Al_2O_3/NiAl(110) prepared via an oxidic and a metallic precursor. In the former case, MoO_x was prepared via direct deposition of MoO_x, while in the latter case, metallic Mo was deposited in an O_2 background. The structure of the resulting catalysts was compared to that of metallic Mo deposited on Al_2O_3/NiAl(110) in the absence of O_2. For directly deposited MoO_x, we observe predominantly point defect nucleation and high particle densities. In contrast, when MoO_x is prepared by deposition of metallic Mo in 5×10^{-7} mbar O_2, we find lower particle densities and preferential nucleation at step edges and domain boundaries, thus reflecting the particle dispersion of metallic Mo. This suggests that the Mo atoms are oxidized typically only after having attached to a stable Mo or MoO_x nucleus. We interpret our findings in terms of the interaction between the deposited material and the support, which is stronger for MoO_x than for Mo. These results demonstrate that the choice of evaporating material crucially influences the catalyst structure and is therefore a useful parameter in tuning the properties of model mixed oxide catalysts.

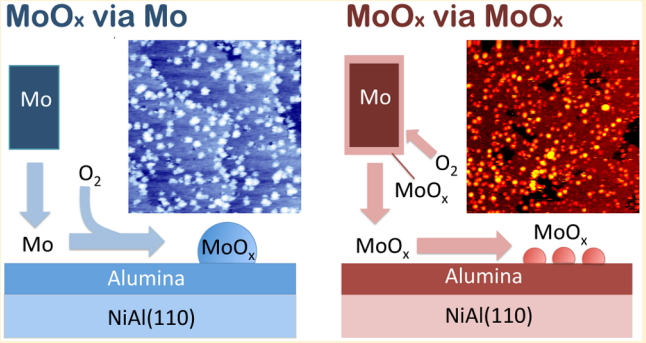

1. INTRODUCTION

Mixed metal oxide catalysts are commonly used in the chemical industry for a wide range of oxidation, reduction, and isomerization reactions.[1] Due to their flexible bonding behavior and variable oxidation state, the rational design of such catalysts remains extremely challenging. The bottom-up approach of surface science allows one to disentangle the multitude of effects that play a role in metal oxide catalysis.

Well-defined model catalysts are typically prepared in ultrahigh vacuum (UHV) by physical vapor deposition of the active phase onto flat oxide single crystals[2−9] or onto thin oxide films supported on single crystals.[10−14] For mixed metal oxide catalysts, the most common procedure is the deposition of metal by electron-beam evaporation in an oxygen background. Metal oxides that are volatile at elevated temperature may also be evaporated directly onto the support, either from an oxide powder source[3] or from an oxidized metal rod or wire.[2]

Formation of the catalyst by these methods usually starts with some form of nucleation and particle growth of the deposited material. There are several parameters that affect the nucleation process,[15,16] such as deposition flux, substrate temperature, and interactions between the deposited material and the support. These provide handles to tune the model catalyst properties. For supported metal clusters and nanoparticles, these parameters have been studied extensively, both theoretically[15,16] and experimentally.[5,17,18] It was shown that high flux and strong metal−support interaction result in formation of a high density of small particles, while the combination of low flux and high temperature yields fewer yet larger particles. As, in general, the surface energy of metals is higher than that of oxides, metals usually form three-dimensional particles on oxide surfaces (Volmer−Weber-type growth)[18,19]

The nucleation and growth stage of mixed metal oxide catalysts is much less studied and shows much larger variation. In some cases, Volmer−Weber-type growth is observed, such as for VO_x[12] and NbO_x[14] on Al_2O_3/NiAl(110). In other cases, particles grow in two-dimensional islands[2] or they do not agglomerate beyond oligomeric clusters.[3,6] Hence, particle sizes and densities may vary strongly, even for similar deposition fluxes and temperatures, depending on the precise choices of supporting and active-phase oxides. Despite the differences in nucleation behavior of supported metals and oxides, the general aspects of nucleation theories developed for metals should also apply to oxides, particularly when nucleation leads to

Received: June 15, 2016
Revised: August 8, 2016
Published: August 10, 2016

DOI: 10.1021/acs.jpcc.6b06040
J. Phys. Chem. C 2016, 120, 19737−19743

sufficiently large particles to satisfy the capillary approximation.[20]

An aspect that has no analogue in the simple case of supported metals is the possibility to deposit different starting materials to make the same metal−support combination. Indeed, mixed metal oxide catalysts can be prepared from deposited metal atoms but also from monomeric or even oligomeric oxide clusters. The large differences between these precursor materials may provide interesting opportunities to tune the properties of the resulting catalyst.

Here, we use X-ray photoelectron spectroscopy (XPS) and scanning tunneling microscopy (STM) to study the effect of the choice of deposited material on the dispersion of MoO_x on Al_2O_3/NiAl(110). We have prepared model catalysts both through the evaporation of MoO_x and through deposition of metallic Mo in an O_2 environment. The resulting catalysts are compared to structures observed after the deposition of metallic Mo on Al_2O_3/NiAl(110). We find that MoO_x prepared via Mo deposition reflects the nucleation behavior of metallic Mo. The observations are discussed in terms of nucleation theory and the timing of oxidation of deposited Mo atoms.

2. METHODS

All experiments were carried out in a home-built UHV apparatus described in detail elsewhere.[21] The system is equipped with a commercial photoelectron spectrometer (SPECS Phoibos), a commercial e-beam evaporator (Oxford Applied Research), standard sample preparation equipment, and a scanning tunneling microscope.

2.1. X-ray Photoelectron Spectroscopy Analysis. All XPS experiments were carried out with the X-ray incidence angle at 54° off normal and electron collection along the surface normal. Peak fitting was performed with the Gaussian/Lorentzian curves implemented in the CasaXPS[22] software package. For fitting of Mo 3d spectra, peak positions were constrained to within 0.1 eV around literature values[23] for Mo^{6+}, Mo^{5+}, Mo^{4+}, and Mo^0. All peak widths (full width at half-maximum, fwhm) were constrained to be equal. The spin−orbit split peak pairs were forced to obey a 3:2 peak area ratio. Fitting of the Ni 3p/Al 2p area was performed with one doublet for the Ni signal and two for Al (Al^0 and Al^{3+}). Again doublets were constrained in area (2:1) and fwhm.

2.2. Sample Preparation. The NiAl(110) sample (Surface Preparation Laboratory)[24] was cleaned by cycles of 1.5 keV Ar^+ bombardment and annealing at 1300 K. Growth of the alumina film was accomplished through three cycles of oxidation at 550 K in a 5×10^{-6} mbar O_2 background (1×10^{-6} mbar O_2 in the last cycle) and subsequent UHV annealing at 1100 K (1050 K in the last cycle).[25] The cleanliness of the film was checked by XPS and STM.

The MoO_x/Al_2O_3/NiAl(110) catalysts were prepared by use of an electron-beam evaporator. All depositions were carried out with the Al_2O_3/NiAl(110) support at room temperature. When MoO_x was deposited, the Mo evaporator rod temperature was set at approximately 1200 K (as determined from the color of the rod), and an O_2 background of 5×10^{-6} mbar was applied. Under these circumstances, volatile MoO_x species are generated on the rod.[2] The mild rod temperature ensures that no metallic Mo evaporates ($P_{vap} = 1.6 \times 10^{-18}$ mbar).[26] Due to the relatively mild oxygen background, we do not expect the formation of oligomeric $(MoO_3)_n$ clusters, which are the predominant gas-phase species when MoO_3 powder is evaporated.[27] We confirmed this by performing a deposition experiment on Au(111), which shows less on-surface oxidation. We observe predominantly Mo^{4+} and Mo^{5+} in XPS. As the formation of oligomeric $(MoO_3)_n$ requires a high surface concentration of Mo^{6+} species on the evaporation rod, we can conclude that this process is unlikely.

For the preparation with Mo as the deposited material, the rod temperature was set at approximately 2000 K in an O_2 background of 5×10^{-7} mbar. Under these conditions, the net oxygen coverage on the rod will be low, while the flux of subliming Mo is high. Hence, Mo should be deposited predominantly in metallic form and become oxidized only after arrival on the Al_2O_3/NiAl(110) support.

2.3. Particle Statistics. Statistics on number density, height, and size of the particles were obtained by use of the Gwyddion software package.[28] The package offers a variety of particle recognition methods, which were cross-checked against each other to ensure robustness of the results with respect to the specific procedure applied. Furthermore, errors found in the automated particle recognition were corrected by hand. By use of the "Watershed" algorithm, apparent agglomerates were separated into individual particles. For statistical analysis, only image segments without steps in the substrate were used.

A combination of STM and XPS results was used to determine the Mo coverage on the sample. The Mo 3d/(Al 2p + Ni 3p) ratio was determined from XPS spectra for all samples. From a series of experiments where metallic Mo was sequentially deposited on the support, we established a linear relationship between the Mo 3d/(Al 2p + Ni 3p) ratio and the coverage obtained from the STM images. To obtain the Mo coverage from an STM image, we calculated the total volume of the particles in the image, with thresholding as the particle detection method. Because STM overestimates the particle height of metallic particles on Al_2O_3/NiAl(110) by approximately 0.3 nm at the sample bias used in this work (−2 V),[13] the recognition threshold was set at this value and the volume was calculated with respect to the horizontal plane defined by the threshold. STM also overestimates the lateral dimensions of the particles. By simple geometrical models, one can establish that this results in a volume overestimation between 2.1× and 17× for the particle sizes investigated here (see Supporting Information). Assuming the tip radius to be of similar size as the particles, we have divided the total volume obtained by the thresholding method by 4. After calibration of the XPS Mo 3d/(Al 2p + Ni 3p) ratio versus STM coverage, a coverage estimate could also be obtained for the MoO_x samples. All coverages are expressed in monolayers of the Mo(110) surface (1 ML corresponds to 1.43×10^{15} Mo atoms·cm^{-2}).

3. MODEL FOR NUCLEATION ON AL_2O_3/NIAL(110)

In contrast to standard nucleation theory, nucleation is strongly heterogeneous for metal clusters on Al_2O_3/NiAl(110). It is governed by three types of nucleation sites:[17] steps, domain boundaries, and point defects of the alumina film. The first two are found to be energetically preferred over the third. However, depending on the deposition parameters and the nature of the deposited material, atoms can become trapped at the point defects before reaching the domain boundaries or steps. When deposition is performed at low sample temperatures or in case of strong deposition material−support interaction, nucleation may even occur almost exclusively at point defects.[10,17] Hence, understanding of the nucleation at point defects is key to understanding the overall nucleation behavior on Al_2O_3/NiAl(110).

DOI: 10.1021/acs.jpcc.6b06040
J. Phys. Chem. C 2016, 120, 19737−19743

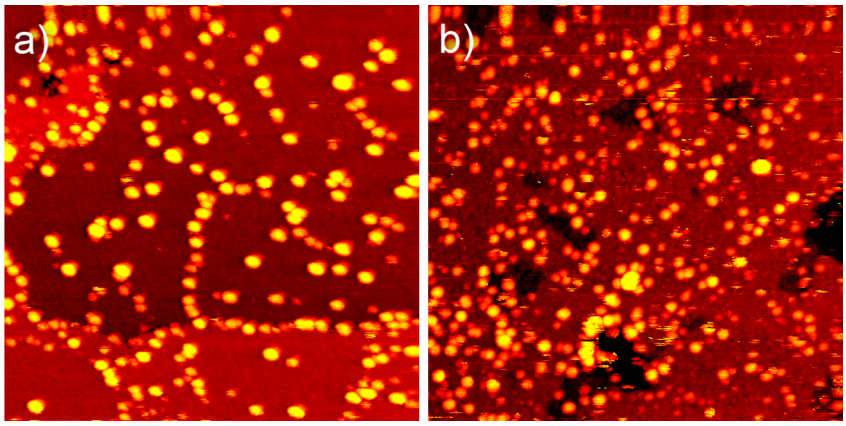

Figure 1. STM images of (a) 0.069 ML metallic Mo, deposited at 1.1×10^{-2} ML/min, and (b) 0.073 ML MoO_x, deposited at 1.5×10^{-3} ML/min. Size 80 nm × 80 nm; sample bias −2 V; tunneling current 50 pA.

A rate equation model for point defect nucleation, showing excellent agreement with experimental data, was put forward by Venables and Harding.[15] For mild sample temperatures and pure point defect nucleation, the only important factor is the average occupation of defect sites by monomers. At very low temperatures, even a single atom is stably bound at a defect site on the time scale relevant to nucleation. In this regime, the particle density is fully determined by the point defect density and will, therefore, be independent of the deposition flux and the nature of the deposited material.[17,18] For metal particles at room temperature, a dimer is usually the smallest stable cluster at point defects on oxide supports.[15] Hence, monomers hop on and off the point defects, leading to not continuously occupied sites. Therefore, it is possible to pass them and move on to other nucleation sites (steps and domain boundaries). The fraction of point defects that is covered in this regime increases with increasing deposition flux and increasing trapping energy. The latter is the energy gained by adsorption of a deposited monomer at a point defect with respect to a regular terrace site. An increase in diffusion rate will lower the fraction of occupied point defects.

Both diffusion rate and trapping energy can be expected to depend on the interaction strength between deposited material and support. Hence, the interaction strength may be a useful parameter to understand trends as a function of the choice of deposited material. For metals, the heat of formation of the highest metal oxide is often used as an indicator for metal−support interactions. Indeed, the average particle size and particle density of metals deposited on Al_2O_3/NiAl(110)[17] were found to correlate with that energy.

An important factor in the description above is the point defect density, for which an STM or XPS characterization is unfortunately not available. However, electron paramagnetic resonance[18] and cathodoluminescence[29] experiments have proven their existence, and comparative nucleation studies have estimated their density to be on the order of 1×10^{13} cm^{-2}.[30] It was not established directly whether this value is reproducible, yet from the trend observed for different metals on Al_2O_3/NiAl(110) produced in various laboratories,[13,17,18,31] we infer that the point defect density must be reproduced quite well. We rationalize this observation by the fact that the point defects in Al_2O_3/NiAl(110) originate from imperfections in the crystallinity of the alumina film and not from loss of oxygen during annealing, such as in the case of TiO_2(110).[32]

4. RESULTS AND DISCUSSION

With the description from section 3 in mind, we will analyze the dispersion of MoO_x and Mo particles on Al_2O_3/NiAl(110), prepared via the two different routes described in section 2.

4.1. Nucleation of Metallic Mo and MoO_x. In order to establish the nucleation characteristics of Mo atoms and MoO_x species, a series of experiments was conducted in which various amounts of Mo (without O_2 background) and MoO_x (via MoO_x deposition) were deposited onto the Al_2O_3/NiAl(110) support. Figure 1 compares the results of both procedures through two STM images. It is clear that even at the qualitative level there are profound differences.

Metallic Mo, like most metals on Al_2O_3/NiAl(110), strongly decorates the step edges. Furthermore, lines of particles are visible on the terraces, indicating that the domain boundaries are also decorated. However, this effect is not as pronounced as for other metals such as Pd and Rh.[13,17,18,31] The clear decoration of steps and domain boundaries shows that the average occupation of point defects was low during the deposition, indicating a mild interaction between deposited material and support. Still, the interaction is stronger than for many other metals, such as Pd, Rh, and Cu,[13,17,18,31] as can be expected from the comparatively high heat of formation of MoO_3.[33]

The MoO_x particles have an entirely different dispersion. They show no clear preference for steps or domain boundaries. This is similar to VO_x[12] and NbO_x[14] on Al_2O_3/NiAl(110) and to metals on this substrate when deposited at 90 K.[17] The lack of step edge/domain boundary decoration indicates that the interaction of MoO_x with the Al_2O_3/NiAl(110) support is much stronger than that of metallic Mo. Mo^{6+} is the dominant oxidation state found for the MoO_x particles (see Supporting Information). This is a higher oxidation state than the Mo^{4+} and Mo^{5+} deposited under these conditions (see section 2), which can be taken as evidence for strong on-surface oxidation during the deposition. Note that the deposition flux was larger for Mo than for MoO_x. Hence, the intrinsic differences between the nucleation behavior of Mo and MoO_x may be even larger than those observed here.

Figure 2 shows the observed particle height distributions for metallic Mo and MoO_x, and their dependence on the Mo coverage. Note that the observed height will in both cases deviate from the actual topographic height, since STM probes the local density of states rather than atomic positions. The alumina film has a semiconducting character. When measuring

DOI: 10.1021/acs.jpcc.6b06040
J. Phys. Chem. C 2016, 120, 19737−19743

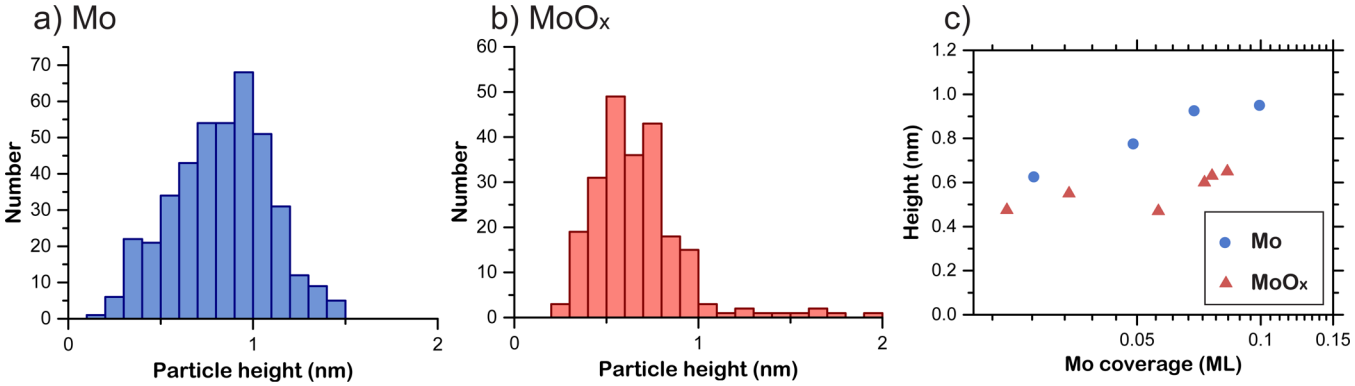

Figure 2. Particle height data of 0.069 ML Mo (deposited at 1.1×10^{-2} ML/min) and 0.076 ML MoO_x (deposited at 1.5×10^{-3} ML/min) from STM images recorded at −2 V. (a, b) Observed height distributions. (c) Peak positions of height distributions as a function of coverage.

on the terrace at mild sample voltage, the tunneling electrons originate from the metallic NiAl(110) rather than from the alumina film.[13,18] For this reason, the particle height of metal particles on Al_2O_3/NiAl(110) is overestimated when a bias voltage within the band gap of the alumina film is used. At −2 V, this overestimation is approximately 0.3 nm.[13]

The data of metallic molybdenum clearly evidence Volmer−Weber-type growth, as also observed for other metals on Al_2O_3/NiAl(110).[10,13,17] The comparatively low particle height fits well with the relatively strong Mo−alumina interaction expected from the high heat of formation of MoO_3.[33] Notice that if one would correct for the overestimation of height, some of the particles are located inside the oxide film. This is likely related to oxidation of some of the very small particles. When sufficiently oxidized, MoO_x particles typically display a band gap.[34] This may decrease their observed height. Indeed, the XPS spectra indicate a small amount of oxidized Mo (see Supporting Information). This oxidation could result either from transfer of electron density to the oxygen atoms of the alumina film or from oxidation by the residual gas background in the UHV system.

When interpreting the data from the MoO_x deposition in Figure 2b, one has to take into account that both the alumina film and the MoO_x particles themselves have a semiconducting character.[34] The true particle height is therefore not immediately clear. Indeed, when the sample bias is decreased to −1 V, many particles "disappear" from the STM image. Nonetheless, the height information can be used to establish the growth mode of MoO_x. The width of the height distribution in Figure 2b can be caused either by particles of varying height or by particles bound in different ways to the support, resulting in different semiconducting character. If the latter were correct, one may expect the observed particle height to decrease with increasing coverage. The reason is that the band gap of MoO_x typically increases when its coordination number increases.[34] This can be expected to occur when the particles grow. From Figure 2c it is clear that the observed particle height increases rather than decreases. Hence, MoO_x also shows Volmer−Weber growth.

From the literature,[13,35−37] we expect that no mixing occurs between the MoO_x particles and the alumina film. First, MoO_x/alumina catalysts are often heated in the chemical industry, but the formation of mixed Mo−alumina oxides is not observed.[35] Second, Al_2O_3/NiAl(110) appears less prone to formation of mixed oxides than other forms of alumina. Cobalt aluminates are commonly observed in the chemical industry,[35] but no compound formation was observed upon Co deposition on Al_2O_3/NiAl(110),[13,36] even at elevated temperatures and in an oxygen environment. Similarly, a theoretical study on vanadia deposition on Al_2O_3/NiAl(110) concluded that extreme conditions would be required for mixing reactions to occur.[37]

In Figure 3a, the particle density of metallic Mo and MoO_x is depicted as a function of Mo coverage. The higher slope of MoO_x can be explained by its stronger support interaction. Such increased support interaction leads to a higher monomer occupation of the point defects in the film, thus increasing the odds of forming a new nucleus with respect to attaching to a pre-existing one. Again, the observed differences between metallic and oxidic Mo may be decreased by the higher flux used for metallic Mo.

Figure 3b shows literature data of nucleation studies with V,[10] VO_x,[12] and NbO_x[14] on Al_2O_3/NiAl(110). For easy comparison to literature, we have chosen to express all coverages in terms of monolayers of each metal's (110) plane. The density of atoms per square centimeter is obtained simply by multiplying the coverage by the atomic density of the corresponding (110) surface [1.43×10^{15} cm^{-2} for Mo(110), 1.54×10^{15} cm^{-2} for V(110), and 1.84×10^{15} cm^{-2} for Nb(110)].

In comparison with VO_x, MoO_x has a lower particle density, which leads to the conclusion that the support−MoO_x interaction is not strong enough to create full coverage of MoO_x monomers on the point defects during deposition. This means that the nucleation density of MoO_x will be dependent on deposition flux at room temperature. As the flux in our experiments was roughly 2 orders of magnitude lower than in the case of VO_x, the observed differences in nucleation density may be larger than in the case of equal flux. NbO_x, which was deposited roughly 1 order of magnitude faster than MoO_x, behaves similarly to MoO_x. One can therefore expect that the MoO_x density on pristine Al_2O_3/NiAl(110) should reach a plateau value at 2×10^{13} cm^{-2}, similar to the cases of NbO_x and VO_x. Due to particle-catalyzed film growth during O_2 exposure, which was also observed for other metals,[12,14,36] we could not obtain data of sufficient quality at higher coverages to establish this.

Note that the plateau value of 2×10^{13} nuclei·cm^{-2} is higher than the literature value of 1×10^{13} point defects·cm^{-2}. This could be explained either by the existence of point defects of a type that has thus far not been probed or by partial homogeneous nucleation. Since VO_x and NbO_x reach the

DOI: 10.1021/acs.jpcc.6b06040
J. Phys. Chem. C 2016, 120, 19737−19743

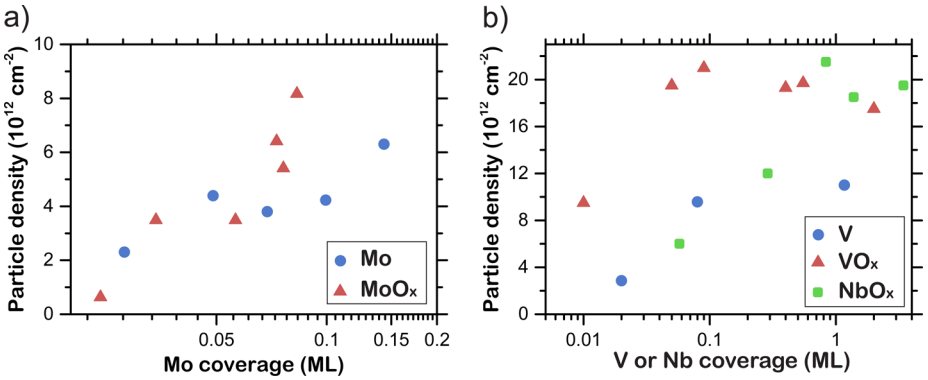

Figure 3. Coverage dependence of particle density. (a) Metallic Mo deposited at 1.1×10^{-2} to 1.5×10^{-2} ML/min and MoO_x deposited at 1.0×10^{-3} to 1.5×10^{-3} ML/min. (b) Literature data for metallic V deposited at ±0.35 ML/min,[10] VO_x deposited at 0.36 ML/min,[12] and NbO_x deposited at 2.8×10^{-2} ML/min.[14] All coverages are expressed in terms of the metal's (110) plane. All depositions were performed with the sample at room temperature.

same plateau level, it can be expected that the former is the more likely explanation.

4.2. Preparation of MoO_x via Mo. Based on an understanding of the nucleation properties of Mo and MoO_x, we can study the dispersion of MoO_x prepared via deposition of metallic Mo in an O_2 background (on-surface oxidation). Figure 4 shows the result of this procedure at a coverage of 0.21

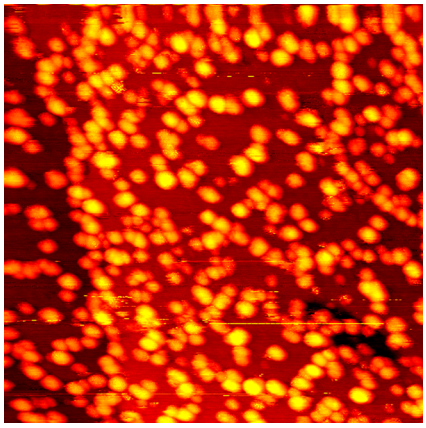

Figure 4. STM image of 0.21 ML MoO_x prepared by deposition of metallic Mo at 1.2×10^{-2} ML/min in 5×10^{-7} mbar O_2. Size 80 nm × 80 nm; sample bias −2 V; tunneling current 50 pA.

ML. Clearly, the step edges are strongly decorated, similar to the case of Mo nucleation in the absence of an O_2 background. Notice also, particularly in the top right of the image, that lines of particles are visible on the terraces, indicating decoration of the domain boundaries. Again, this strongly resembles the behavior of metallic Mo.

The resemblance between nucleation behavior of metallic Mo and of MoO_x prepared via metallic Mo also extends to the particle density. At 0.21 ML, we found a density of 6.9×10^{12} cm^{-2}, which clearly fits in the trend of metallic Mo, but is roughly half the value expected for MoO_x nucleation.

The observations above can be explained by the timing of on-surface oxidation of molybdenum. When the newly arrived Mo atoms become oxidized only after diffusing over the surface and attaching to a stable nucleus, their nucleation behavior will reflect that of metallic Mo atoms. Indeed, XPS spectra show that MoO_x particles prepared via Mo are less strongly oxidized than those prepared via MoO_x evaporation (see Supporting Information), thus showing that the process of Mo oxidation is kinetically hindered at room temperature. When 0.10 ML of metallic Mo is deposited onto the substrate without O_2 background and subsequently exposed to oxygen, very little oxidation occurs. Therefore, oxidation and particle growth must occur hand in hand. Each newly arriving Mo atom is oxidized before its number of Mo neighbors increases to such an extent that oxidation becomes kinetically inhibited.

It should be noted at this point that the VO_x[12] and NbO_x[14] catalysts we have been comparing to were prepared by depositing metallic V and Nb in an oxygen background. The vanadium data (see Figure 3b) show a clear difference in the nucleation behavior of metal[10] and oxide; hence the vanadium atoms arriving on the surface in an O_2 background were oxidized before attaching to a stable nucleus. The difference in the behavior of Mo and V can be explained by the higher reactivity toward oxygen of vanadium.[33] This results in a slower diffusion of vanadium on the support and possibly also in a higher sticking probability of oxygen. The higher particle density of metallic vanadium versus metallic molybdenum (see Figure 3) indeed seems to support such slower diffusion, but the difference in deposition flux makes it inappropriate to compare these observations fully quantitatively.

Our results show that the timing of oxidation during metal oxide particle growth has a large influence on the resulting model catalyst. The origin of this is that isolated metal oxide units often have a very different interaction with the support than metal atoms. In the case of Mo, the interaction is clearly stronger for the oxide units than for the metal atoms. In order to obtain small particles, one therefore should choose to deposit MoO_x directly onto the support. For large particles, one should rather deposit metallic Mo in an oxygen background. Although not explored here, changing the O_2 pressure should allow one to continuously change the ratio of metallic Mo atoms and isolated MoO_x units diffusing on the surface, thus providing more continuous control over the particle size.

5. CONCLUSION

We have studied the nucleation behavior of metallic Mo and MoO_x prepared either via direct deposition of MoO_x or via deposition of metallic Mo in an O_2 background. We find that metallic molybdenum behaves similar to other reactive metals, with three-dimensional particles nucleating at the oxide film's point defects as well as on its domain boundaries and steps.

DOI: 10.1021/acs.jpcc.6b06040
J. Phys. Chem. C 2016, 120, 19737−19743

The average particle size and nucleation density fit well with the trends for other metals, based on their heat of highest oxide formation.

When MoO_x is prepared by direct deposition of in situ generated MoO_x, we find a much stronger support interaction than in the case of metallic Mo, resulting in a higher particle density and a domination of point defect nucleation. Nonetheless, we observe that the particles grow in a three-dimensional mode.

When MoO_x is prepared by deposition of metallic Mo in a 5×10^{-7} mbar O_2 background, the nucleation behavior clearly reflects the behavior of the metal rather than the oxide. This is explained by the timing of oxidation of the molybdenum on the surface. It is found that Mo atoms arriving on the surface are typically oxidized only after attaching to a stable nucleus.

We have thus established that the choice of evaporating material is a useful parameter to tune model mixed metal oxide catalyst properties. As an outlook, we may expect that changing the O_2 pressure should allow one to continuously change the ratio of metallic Mo atoms and isolated MoO_x units diffusing on the surface, thus providing continuous control over the particle size.

■ ASSOCIATED CONTENT

Supporting Information

The Supporting Information is available free of charge on the ACS Publications website at DOI: 10.1021/acs.jpcc.6b06040.

Additional text and equations and five figures showing modeling of volume overestimation of particles by STM and XPS analysis of Mo and MoO_x samples (PDF)

■ AUTHOR INFORMATION

Corresponding Author

*E-mail mom@physics.leidenuniv.nl; tel +31-(0)715275602.

Notes

The authors declare no competing financial interest.

■ ACKNOWLEDGMENTS

This project was financially supported by a Dutch SmartMix grant and by NIMIC partner organizations through NIMIC, a public−private partnership. I.M.N.G. acknowledges the Dutch organization for scientific research for her Veni fellowship. We thank professor Anja Sjåstad for fruitful discussions.

■ REFERENCES

(1) Fierro, J. L. G. *Metal Oxides: Chemistry and Applications*; CRC Press: Boca Raton, FL, 2006.

(2) Bamroongwongdee, C.; Bowker, M.; Carley, A. F.; Davies, P. R.; Davies, R. J.; Edwards, D. Fabrication of Complex Model Oxide Catalysts: Mo Oxide Supported on Fe3O4(111). *Faraday Discuss.* **2013**, *162*, 201−212.

(3) Bondarchuk, O.; Huang, X.; Kim, J.; Kay, B. D.; Wang, L.-S.; White, J. M.; Dohnálek, Z. Formation of Monodisperse (WO3)3 Clusters on TiO 2(110). *Angew. Chem., Int. Ed.* **2006**, *45*, 4786−4789.

(4) Desikusumastuti, A.; Laurin, M.; Happel, M.; Qin, Z.; Shaikhutdinov, S.; Libuda, J. Strong Size Effects in Supported Ionic Nanoparticles: Tailoring the Stability of NO X Storage Catalysts. *Catal. Lett.* **2008**, *121*, 311−318.

(5) Galhenage, R. P.; Yan, H.; Tenney, S. A.; Park, N.; Henkelman, G.; Albrecht, P.; Mullins, D. R.; Chen, D. A. Understanding the Nucleation and Growth of Metals on TiO 2: Co Compared to Au, Ni, and Pt. *J. Phys. Chem. C* **2013**, *117*, 7191−7201.

(6) Karslıoğlu, O.; Song, X.; Kuhlenbeck, H.; Freund, H. Mo +TiO2(110) Mixed Oxide Layer: Structure and Reactivity. *Top. Catal.* **2013**, *56*, 1389−1403.

(7) Kim, H. Y.; Lee, H. M.; Pala, R. G. S.; Metiu, H. Oxidative Dehydrogenation of Methanol to Formaldehyde by Isolated Vanadium, Molybdenum, and Chromium Oxide Clusters Supported on Rutile TiO 2 (110). *J. Phys. Chem. C* **2009**, *113*, 16083−16093.

(8) Park, J. B.; Graciani, J.; Evans, J.; Stacchiola, D.; Ma, S.; Liu, P.; Nambu, A.; Sanz, J. F.; Hrbek, J.; Rodriguez, J. A. High Catalytic Activity of Au/CeOx/TiO2(110) Controlled by the Nature of the Mixed-Metal Oxide at the Nanometer Level. *Proc. Natl. Acad. Sci. U. S. A.* **2009**, *106*, 4975−4980.

(9) Rodriguez, J. A.; Stacchiola, D. Catalysis and the Nature of Mixed-Metal Oxides at the Nanometer Level: Special Properties of MOx/TiO2(110) {M= V, W, Ce} Surfaces. *Phys. Chem. Chem. Phys.* **2010**, *12*, 9557−9565.

(10) Bäumer, M.; Biener, J.; Madix, R. J. Growth, Electronic Properties and Reactivity of Vanadium Deposited onto a Thin Alumina Film. *Surf. Sci.* **1999**, *432*, 189−198.

(11) Desikusumastuti, A.; Qin, Z.; Staudt, T.; Happel, M.; Lykhach, Y.; Laurin, M.; Shaikhutdinov, S.; Libuda, J. Controlling Metal/oxide Interactions in Bifunctional Nanostructured Model Catalysts: Pd and BaO on Al2O3/NiAl(1 1 0). *Surf. Sci.* **2009**, *603*, L9−L13.

(12) Magg, N.; Giorgi, J. B.; Schroeder, T.; Bäumer, M.; Freund, H.-J. Model Catalyst Studies on Vanadia Particles Deposited onto a Thin-Film Alumina Support - 1. Structural Characterization. *J. Phys. Chem. B* **2002**, *106*, 8756−8761.

(13) Napetschnig, E.; Schmid, M.; Varga, P. Pd, Co and Co-Pd Clusters on the Ordered Alumina Film on NiAl(1 1 0): Contact Angle, Surface Structure and Composition. *Surf. Sci.* **2007**, *601*, 3233−3245.

(14) Uhl, A.; Sainio, J.; Lahtinen, J.; Shaikhutdinov, S.; Freund, H.-J. Preparation and Structure of Alumina Supported Niobia Model Catalysts. *Surf. Sci.* **2007**, *601*, 5605−5610.

(15) Venables, J. A.; Harding, J. H. Nucleation and Growth of Supported Metal Clusters at Defect Sites on Oxide and halide(001) Surfaces. *J. Cryst. Growth* **2000**, *211*, 27−33.

(16) Michely, T.; Krug, J. *Islands, Mounds and Atoms: Patterns and Processes in Crystal Growth Far from Equilibrium*; Springer-Verlag: Berlin and Heidelberg, Germany, 2004; DOI: 10.1007/978-3-642-18672-1.

(17) Bäumer, M.; Frank, M.; Heemeier, M.; Kühnemuth, R.; Stempel, S.; Freund, H.-J. Nucleation and Growth of Transition Metals on a Thin Alumina Film. *Surf. Sci.* **2000**, *454-456*, 957−962.

(18) Bäumer, M.; Freund, H.-J. Metal Deposits on Well-Ordered Oxide Films. *Prog. Surf. Sci.* **1999**, *61*, 127−198.

(19) Naidich, J. V. The Wettability of Solids by Liquid Metals. *Prog. Surf. Membr. Sci.* **1981**, *14*, 353−484.

(20) Julin, J.; Napari, I.; Merikanto, J.; Vehkamäki, H. A Thermodynamically Consistent Determination of Surface Tension of Small Lennard-Jones Clusters from Simulation and Theory. *J. Chem. Phys.* **2010**, *133*, 044704.

(21) Herbschleb, C. T.; van der Tuijn, P. C.; Roobol, S. B.; Navarro, V.; Bakker, J. W.; Liu, Q.; Stoltz, D.; Cañas-Ventura, M. E.; Verdoes, G.; van Spronsen, M. a; et al. The ReactorSTM: Atomically Resolved Scanning Tunneling Microscopy under High-Pressure, High-Temperature Catalytic Reaction Conditions. *Rev. Sci. Instrum.* **2014**, *85*, 083703.

(22) Fairley, N. *CasaXPS*, v 2.3; SPECS, Berlin, 1999.

(23) Spevack, P. A.; McIntyre, N. S. A Raman and XPS Investigation of Supported Molybdenum Oxide Thin Films. 2. Reactions with Hydrogen Sulfide. *J. Phys. Chem.* **1993**, *97*, 11031−11036.

(24) Surface Preparation Laboratory. Penningweg 69F, 1507 DE Zaandam, The Netherlands; https://www.spl.eu/.

(25) Jaeger, R. M.; Kuhlenbeck, H.; Freund, H.; Wuttig, M.; Hoffmann, W.; Franchy, R.; Ibach, H. Formation of a Well-Ordered Aluminium Oxide Overlayer by Oxidation of NiAl (110). *Surf. Sci.* **1991**, *259*, 235−252.

DOI: 10.1021/acs.jpcc.6b06040
J. Phys. Chem. C 2016, 120, 19737−19743

(26) Alcock, C. B.; Itkin, V. B.; Horrigan, M. K. Vapor-Pressure Equations for the Metallic Elements - 298−2500 K. *Can. Metall. Q.* **1984**, *23*, 309.
(27) Rousseau, R.; Dixon, D. A.; Kay, B. D.; Dohnálek, Z. Dehydration, Dehydrogenation, and Condensation of Alcohols on Supported Oxide Catalysts Based on Cyclic $(WO_3)_3$ and $(MoO_3)_3$ Clusters. *Chem. Soc. Rev.* **2014**, *43*, 7664−7680.
(28) Nečas, D.; Klapetek, P. Gwyddion: An Open-Source Software for SPM Data Analysis. *Open Phys.* **2012**, *10*, 181−188.
(29) Adelt, M.; Nepijko, S.; Drachsel, W.; Freund, H.-J. Size-Dependent Luminescence of Small Palladium Particles. *Chem. Phys. Lett.* **1998**, *291*, 425−432.
(30) Frank, M.; Bäumer, M. From Atoms to Crystallites: Adsorption on Oxide-Supported Metal Particles. *Phys. Chem. Chem. Phys.* **2000**, *2*, 3723−3737.
(31) Worren, T.; Højrup Hansen, K.; Lægsgaard, E.; Besenbacher, F.; Stensgaard, I. Copper Clusters on Al2O3/NiAl(110) Studied with STM. *Surf. Sci.* **2001**, *477*, 8−16.
(32) Wendt, S.; Schaub, R.; Matthiesen, J.; Vestergaard, E. K.; Wahlström, E.; Rasmussen, M. D.; Thostrup, P.; Molina, L. M.; Lægsgaard, E.; Stensgaard, I.; et al. Oxygen Vacancies on TiO2(1 1 0) and Their Interaction with H2O and O2: A Combined High-Resolution STM and DFT Study. *Surf. Sci.* **2005**, *598*, 226−245.
(33) Chase, M. W. *NIST−JANAF Tables, 4th ed.*; National Institute of Standards and Technology, Gaithersburg, MD, 1998; kinetics.nist.gov/janaf/.
(34) Mosqueira, L.; Gómez, S. A.; Fuentes, G. A. Characterization of MoO_x Species on Al_2O_3, Y and ZSM-5 Zeolites during Thermally Activated Solid−solid Synthesis. *J. Phys.: Condens. Matter* **2004**, *16*, S2319−S2327.
(35) Lipsch, J. M. J. G.; Schuit, G. C. A. The CoO-MoO3-Al2O3 Catalyst. *J. Catal.* **1969**, *15*, 174−178.
(36) Nowitzki, T.; Carlsson, A. F.; Martyanov, O.; Naschitzki, M.; Zielasek, V.; Risse, T.; Schmal, M.; Freund, H.-J.; Bäumer, M. Oxidation of Alumina-Supported Co and Co - Pd Model Catalysts for the Fischer - Tropsch Reaction. *J. Phys. Chem. C* **2007**, *111*, 8566−8572.
(37) Brazdova, V.; Ganduglia-Pirovano, M. V.; Sauer, J. Vanadia Aggregates on an Ultrathin Aluminium Oxide Film on NiAl(110). *J. Phys. Chem. C* **2010**, *114*, 4983−4994.

DOI: 10.1021/acs.jpcc.6b06040
J. Phys. Chem. C 2016, 120, 19737−19743